Supporting Information

Weitz et al. 10.1073/pnas.1309915111

SI Text

Determining Processing Competency of Pri-miRNAs in Cells. We tested whether the reporter assay can distinguish a processing-incompetent primary transcript of microRNA (pri-miRNA) mutant from the wild type. Pairing interaction around the Drosha cleavage sites in pri-mRNAs has been shown to be critical for processing (1). We mutated four residues around the 5′ Drosha cleavage site in the pri-miR-9-1 reporter to generate the M1 construct (Fig. S4*A*). Cotransfection of the M1 reporter with pN-flag-DGCR8 did not show the large increase in slope that was observed for the wild type (Fig. S4 *B* and *C*). Cotransfection with ΔCTT also did not exhibit significant changes. The lack of changes in processing of pri-miR-9-1 M1 by ectopic expression of N-flag-DGCR8 was confirmed by measurements of mCherry–pri-miR-9–1 fusion and eYFP mRNA levels using quantitative RT-PCR (qRT-PCR) (Fig. S4*D*). These results indicate that our reporter assay detects legitimate pri-miRNA cleavage events and may be used to examine processing competency of pri-miRNAs in cells.

SI Materials and Methods

Reagents. Succinylacetone (synonym 4,6-Dioxoheptanoic acid), doxycycline, and horse skeletal muscle apomyoglobin were from Sigma-Aldrich. Hemin was from MP Biomedicals. δ-Aminolevulinic acid (δ-ALA) was from either MP Biomedicals or Frontier Scientific. The siRNAs were purchased from Dharmacon, Thermo Scientific. The 4-^{14}C-aminolevulinic acid was a gift from Li Zhang (University of Texas at Dallas). Mature miR-9 Locked Nucleic Acids (LNA) probe was obtained from Exiqon.

Vectors and Cloning. The pri-miRNA processing reporters were engineered based on the bidirectional tetracycline-inducible vector containing mCherry and eYFP (pTRE-BI-red/yellow), both fused to an N-terminal nuclear localization signal sequence (2). Fragments of pri-miR-9-1 (143 nt) and pri-miR-30a (148 nt) were PCR-amplified from human genomic DNA. The primers were as follows with the ClaI and NotI cloning sites underlined: pri-miR-9-1 forward (ACCATCGATGGCTGCGTGGAAGAGGCGG), pri-miR-9-1 reverse (TGCAGCGGCCGCCTGCAGCCCCTCTGCGCAGT), pri-miR-30a forward (ACCATCGATGGAAAGAAGGTATATTGCT), pri-miR-30a reverse (TGCAGCGGCCGCAAACAAGATAATTGCTCCT).

The amplified pri-miRNAs were initially cloned into the ptre2hyg-HA vector (Clontech) between the ClaI and NotI sites for the purpose of a different study. The pri-miRNAs were subsequently excised using ClaI and SalI and inserted into pTRE-BI-red/yellow. The pri-miR-9-1 M1 mutant was made using the QuikChange site-directed mutagenesis protocol (Qiagen). Mutagenesis of N-flag-DGCR8 and NC1 expression constructs was carried out using the standard four-primer PCR method. The RNA- and protein-coding sequences of all plasmids were confirmed by sequencing.

Cell Culture and Transfection. The HeLa Tet-On cell line was purchased from Clontech. HeLa Tet-On cells were cultured in DMEM (Life Technologies) with 5% Tet-system approved FBS (Clontech) in 5% CO_2 at 37 °C. For transfections without siRNAs, 4.8×10^5 cells were seeded on 35-mm glass-bottom plates. The following day, cells were transfected with 0.4 μg of total DNA or 0.8 μg for low expression constructs using the Effectene reagent (Qiagen). Cells were immediately induced with 2 μg/mL doxycycline and imaged 18–24 h later unless specified otherwise. Media with phenol red were used for transfection and induction and were exchanged for a clear medium without the dye and containing 2 μg/mL doxycycline immediately before imaging.

Cotransfection of reporter and siRNAs was performed using the DharmaFECT Duo transfection reagent (Thermo Scientific) following the manufacturer's instructions. The final concentrations of siRNA and plasmid were 100 nM and 2 μg/mL, respectively. The sequence of siDGCR8-1 was the same as reported by Kim and coworkers (3). Cells were passaged 1 d posttransfection, plated on 35-mm glass-bottom plates, and 4 h later induced with 2 μg/mL doxycycline. Cells were imaged 18–24 h postinduction.

Heme-depleted media was made by treating Tet-system approved FBS with 0.1 M ascorbic acid for 2 h (4). The absorbance spectrum of the FBS was recorded at the beginning and throughout the treatment to monitor the disappearance of the 405-nm heme peak. The ascorbic acid was removed by dialyzing against 1 L of phosphate buffered saline (PBS, containing 137 mM NaCl, 2.7 mM KCl, 10 mM Na_2HPO_4, and 1.8 mM KH_2PO_4) at room temperature using dialysis tubing with a molecular mass cutoff of 12,500 Da twice for 1 h each round. Heme-depleted FBS was added to DMEM, and the medium was sterile-filtered. Cells were cultured in heme-depleted media for 24 h and split into either six-well plates or glass-bottom imaging plates. For pri-miRNA processing reporter assays, cells were transfected with Effectene. Either 1 mM succinylacetone (dissolved in water), 10 μM hemin (dissolved in DMSO), or both was added to the cell cultures at the same time as doxycycline. After 10 h, cells were either imaged or lysed for RNA extraction.

Measuring Rates of Heme Biosynthesis. To measure reduction in heme synthesis during succinylacetone/heme treatments, we added to the media 0.4 μCi of 4-^{14}C-aminolevulinic acid and 20 μM unlabeled δ-ALA. After 10 h, cells were washed twice with PBS, scraped into a 2-mL tube, and spun down at 13,226 × *g* for 1 min. Cells were resuspended in 0.3 mL of heme extraction buffer containing 80% (vol/vol) acetone and 0.5 M HCl. Then, 1.2 mL of diethyl ether was added, and the cells were spun down at 13,226 × *g* for 5 min at 4 °C. Two additional rounds of extraction with 2 M HCl were performed, and the final aqueous layer was added to a scintillation vial and allowed to evaporate overnight. The following day, 5 mL of scintillation fluid was added, and the amounts of ^{14}C-labeled heme were measured using a Beckman LS6500 liquid scintillation counter. Three biological replicates were performed, and the counts were normalized to the average of "no-treatment" samples.

Imaging and Analysis. All imaging was performed using a Nikon Eclipse Ti microscope equipped with an EMCCD camera (Andor iXon). We used a 20× air objective (NA = 0.45, Olympus) and lamp illumination (Nikon) at full power, an exposure time of 100 ms and 0 gain. The fluorescence signal was detected using filter cubes for eYFP (510 ± 10 nm band pass excitation and 535 ± 15 nm band pass emission) and mCherry (535 ± 25 nm band pass excitation and 610 ± 10 nm band pass emission). Images were saved as 16-bit tiff files.

We wrote a program based on the Matlab software package (The MathWorks) for integrating fluorescence intensities of individual cells. To determine the perimeter of individual nucleus (segmentation), our program imports individual pairs of eYFP and mCherry images and converts them to binary maps using user-defined threshold values. A value of 1 in the map indicates that the pixel is inside the nucleus, and 0 indicates outside. We

usually choose threshold values that maximize the number of cells detected. The perimeter of the nucleus is determined for each image separately, and then an adequate perimeter is chosen for the two images based on the following criteria. If the same cell is found in both images, the smaller perimeter is chosen to avoid including cytosols, which sometimes have low fluorescent signals. If a cell is detected in only one image, the perimeter is kept, allowing for very dim cells that are not detected in both images to be included. The center of the final perimeter for each cell is determined. After the nuclear perimeters are determined, further analysis is done on the original images. A background fluorescence value is calculated for each image by averaging the intensities of the pixels outside the identified nuclei. The background is then subtracted from the intensities of all pixels. The total intensity of an individual cell is calculated as the sum of the pixel intensities within the perimeter. Users can use the center coordinates in the output to remove dead cells or multiple cells detected as one object.

A list of total eYFP and mCherry intensities for individual cells was compiled in Microsoft Excel. Scatter plots were made for eYFP versus mCherry signals. The data were sorted based on each point's distance from the origin. Ten percent of the data with the highest intensities were removed, as they tend to dominate and possibly skew the linear fit. The final datasets were imported into Matlab and fit using the curve fit toolbox. *P* values were determined using the linear fit function of PRISM (GraphPad, version 4).

qRT-PCR for RNA Analyses. Total RNAs were extracted using the miRNeasy Mini kit (Qiagen) and were digested on-column using the RNase-free DNase set (Qiagen). The reverse transcription (RT) reactions were set up using SuperScript II (Life Technologies), and the quantitative PCR (qPCR) was performed using Platinum SYBR Green qPCR Supermix-UDG (Life Technologies). Following are a list of primers used for RT and qPCR reactions: mCherry RT (*TGTCAGGCAACCGTATTCACC*GTTCGTACTGTTCCACGA), eYFP RT (*TGTCAGGCAACCGTATTCACC*ACTCCAGCAGGACCATGTGAT), mCherry qPCR forward (ACTACGACGCTGAGGTCAA), eYFP qPCR forward (AAGATCCGCCACAACATCGA), and qPCR reverse for mCherry and eYFP (*TGTCAGGCAACCGTATTCACC).*

To prevent potential plasmid in the RNA samples from interfering with the qPCR reactions, the RT primers were designed to include a 21-nt 5′-overhang (shown above in italics). The qPCR reverse primer sequence was identical to this overhang whereas the forward primers were gene-specific. A three-step qPCR reaction was performed with an annealing temperature of 60 °C. qPCR results were analyzed using the MxPro software (Stratagene). We calculated the ΔC_t values of the mCherry and eYFP transcripts and determined the fold changes by normalizing to the reporter only control.

Mature miR-9 and miR-30a (miR-9-5p and miR-30a-5p in the current miRBase nomenclature) were detected using TaqMan miRNA reverse transcription and miRNA Assay kits (Life Technologies) following the manufacturer's instructions. Ten nanograms of total RNA was used in each reverse transcription. C_t values were subtracted by those of either U6 small nuclear RNA or β-actin mRNA. Fold changes were calculated and normalized to the reporter-only control. DGCR8 expression was detected using a Taqman gene expression assay (Life Technologies), with RT performed using a random primer set and SuperScipt II (Life Technologies). The C_t values were subtracted by those of β-actin mRNA, and the fold change was calculated and was normalized to that of the siCyclophillin control transfection. All *P* values were calculated using a two-tailed Student *t* test except in Fig. 2*B* where a one-tailed *t* test was used.

Northern Blotting. Total RNA samples were prepared using the TriZol reagent (Invitrogen) according to the manufacturer's instructions. RNA quality and relative concentrations were determined using 1% agarose gels. Three to 20 μg of RNAs were loaded onto 15% polyacrylamide gels containing 7 M urea and separated by electrophoresis. RNA was transferred to Hybond-N+ membranes (GE Healthcare) and was cross-linked using UV light. The probe for U6 snRNA is a DNA oligo with the sequence 5′-AACGCTTCACGAATTTGCGT-3′. The probes were 5′-labeled with γ-^{32}P- ATP and were hybridized to membranes in ULTRAhyb-Oligo hybridization buffer (Life Technology) at 42 °C overnight. The membranes were washed and exposed to phosphorimagers. The images were recorded using a Typhoon Variable Mode Imager, and the bands were quantified using the program Quantify One (version 4.4.1; Bio-Rad). The plotting was performed using the program PRISM (version 4.0; GraphPad).

Immunoblotting. HeLa cells were transfected with the wild-type and mutant pN-flag-DGCR8 plasmids using Effectene (Qiagen) following standard protocol. Twenty-four hours posttransfection, cells were washed twice with PBS, scraped into 200 μL of PBS, and pelleted by centrifugation at 1,000 × *g* for 2 min at 4 °C. The PBS was removed, and ∼1×10^6 cells were resuspended in 80 μL of cold Buffer A [10 mM Hepes-KOH (pH 7.9), 1.5 mM $MgCl_2$, 10 mM KCl, 0.5 mM DTT, 0.2 mM phenylmethylsulfonyl fluoride (PMSF)]. Cells were incubated on ice for 10 min and then vortexed for 10 s and pelleted by centrifugation at 16,000 × *g* for 10 s at 4 °C. The supernatant (cytoplasmic fraction) was transferred to a new tube. The pellet was resuspended in 50 μL of Buffer C [20 mM Hepes-KOH (pH 7.9), 25% glycerol, 420 mM NaCl, 1.5 mM $MgCl_2$, 0.5 mM DTT, 0.2 mM PMSF] and incubated on ice for 20 min. Cells were pelleted by centrifugation at 16,000 × *g* for 2 min at 4 °C. The supernatant (nuclear fraction) was transferred to a new tube and processed for immunoblotting following our standard procedure (5). The membranes were first incubated overnight with mouse anti-FLAG antibodies (Sigma; diluted 1:1,000) followed by a 2-h incubation at room temperature with anti-mouse antibodies conjugated with horseradish peroxidase (HRP) (Novagen) (1:30,000 dilution). The membrane was washed thoroughly in PBST (PBS with 0.2% Tween-20), and the ECL Plus Western Blotting Detection System (GE Healthcare) protocol was then used according to the manufacturer's instructions. The images were recorded using chemifluorescence and the Typhoon Variable Mode Imager (GE Healthcare).

Expression, Purification, and Characterization of Recombinant NC1 Proteins. Human NC1 (wild type and mutants) proteins were expressed and purified as previously described (6). Briefly, they were expressed in *Escherichia coli* BL21(DE3) CodonPlus cells (Stratagene) grown in LB media supplemented with 1 mM δ-ALA at the time of induction. These proteins were purified using cation exchange followed by size exclusion chromatography. The purified proteins were stored in a buffer containing 20 mM Tris, pH 8.0, 400 mM NaCl, and 1 mM DTT. Electronic absorption spectra were recorded on a Beckman-Coulter DU800 spectrophotometer at 25 °C.

Heme dissociation and association assays were performed as described (7), in a buffer containing 20 mM Tris, pH 8.0, 400 mM NaCl, and 1 mM DTT. Fe(III) heme-bound NC1 S349A and H354A mutants, at 5.75 and 4.0 μM dimer concentrations, respectively, were incubated at room temperature with eightfold molar excess of apomyoglobin, which has an extremely high affinity for heme, with K_D of 3×10^{-15} M, and serves as a heme sink. Electronic absorption spectra were recorded over a period of 24 h. No heme transfer from NC1 mutants to apomyoglobin was observed. For heme association with the heme-free NC1 mutant dimers, I350A and L353A, 5 μM of the proteins were titrated with up to 10 μM Fe(III) heme, and electronic absorption spectra were recorded. Hemin chloride was converted to Fe(III) heme by dissolving it in 1.4 M NaOH at 10 mM concentration and incubating in the dark at room temperature for >30 min.

This concentrated solution was then diluted in water to give a 100-μM stock solution. No absorption peaks were observed around 450 nm, where the signature DGCR8-Fe(III) heme Soret peak is located.

Sequence Alignment. The following National Center for Biotechnology Information (NCBI) accession numbers were used for the DGCR8 homolog alignment: Human, *Homo sapien* (NCBI accession no. NM_022720); Marmoset, *Callithrix jacchus* (XM_002806547); Dog, *Canis familiaris* (XM_543542.4); Panda, *Ailuropoda melanoleuca* (XM_002920581); Mouse, *Mus musculus* (NM_033324); Chicken, *Gallus gallus* (XM_415079); Frog, *Xenopus laevis* (BC070985); Bat star, *Patiria miniata* (GQ397480.1); Shrimp, *Litopenaeus vannamei* (HQ692889.1); Fly, *Drosophila melanogaster* (NM_143622); Pea aphid, *Acyrthosiphon pisum* (NW_003383706.1); and Worm, *Caenorhabditis elegans* (NM_060373).

1. Lee Y, et al. (2003) The nuclear RNase III Drosha initiates microRNA processing. *Nature* 425(6956):415–419.
2. Mukherji S, et al. (2011) MicroRNAs can generate thresholds in target gene expression. *Nat Genet* 43(9):854–859.
3. Han J, et al. (2004) The Drosha-DGCR8 complex in primary microRNA processing. *Genes Dev* 18(24):3016–3027.
4. Ye W, Zhang L (2004) Heme deficiency causes apoptosis but does not increase ROS generation in HeLa cells. *Biochem Biophys Res Commun* 319(4):1065–1071.
5. Gong M, et al. (2012) Caspases cleave and inhibit the microRNA processing protein DiGeorge Critical Region 8. *Protein Sci* 21(6):797–808.
6. Faller M, Matsunaga M, Yin S, Loo JA, Guo F (2007) Heme is involved in microRNA processing. *Nat Struct Mol Biol* 14(1):23–29.
7. Barr I, et al. (2011) DiGeorge critical region 8 (DGCR8) is a double-cysteine-ligated heme protein. *J Biol Chem* 286(19):16716–16725.

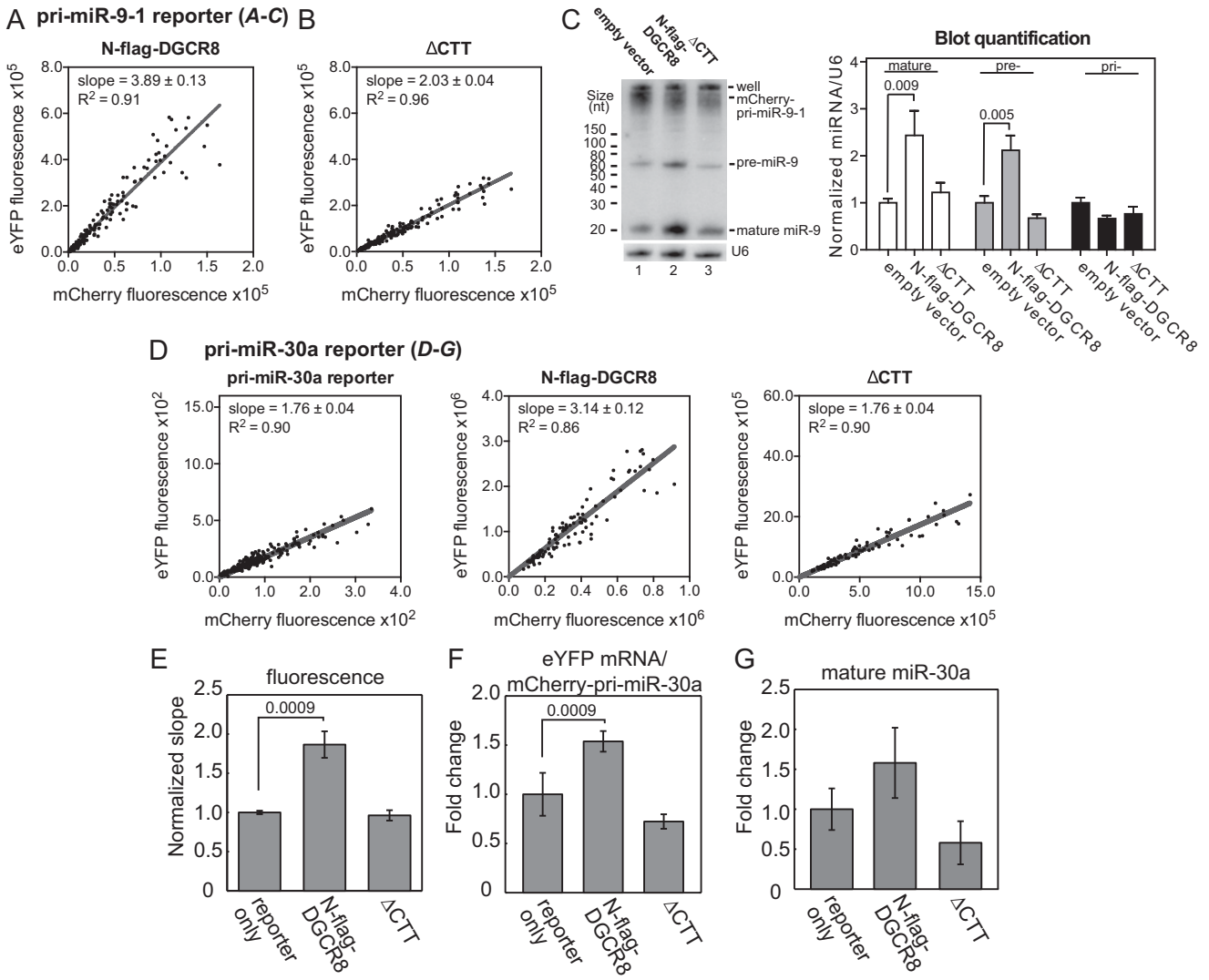

Fig. S1. Validation of the pri-miR-9–1 and pri-miR-30a reporters. (*A*–*C*) Validation of the pri-miR-9-1 reporter. Shown are additional data for the experiments described in Fig. 1*E*. Scatter plots of eYFP vs. mCherry fluorescent intensities of individual cells from cotransfection of the pri-miR-9-1 reporter with either wild-type N-flag-DGCR8 expression plasmid (*A*) or the ΔCTT mutant (*B*). The lines are from linear regression, with slope and R^2 shown on the graph. The ratio of *y* and *x* axes was set at 4:1 for all scatter plots. (*C*) Northern blotting analyses of total RNA samples. The pri-, pre-, and mature miR-9 intensities, after normalization by those of U6 snRNA, are indicated on the graph (mean ± SD, $n = 3$). (*D*–*G*) Validation of the pri-miR-30a reporter. HeLa cells were transfected with the pri-miR-30a reporter either alone or with N-flag-DGCR8 expression plasmid (wild type or ΔCTT). (*D*) Scatter plots of eYFP vs. mCherry fluorescence intensities of individual cells. The lines are from linear regression, with slope and R^2 shown on the graph. (*E*) Normalized eYFP/mCherry fluorescence slopes. Error bars represent 95% confidence interval (CI) of the linear fit. (*F* and *G*) qRT-PCR analyses of the mCherry-pri-miR-30a fusion RNA (*F*) and mature miR-30a (*G*). Error bars represent SD ($n = 3$). *P* values are labeled on the graphs.

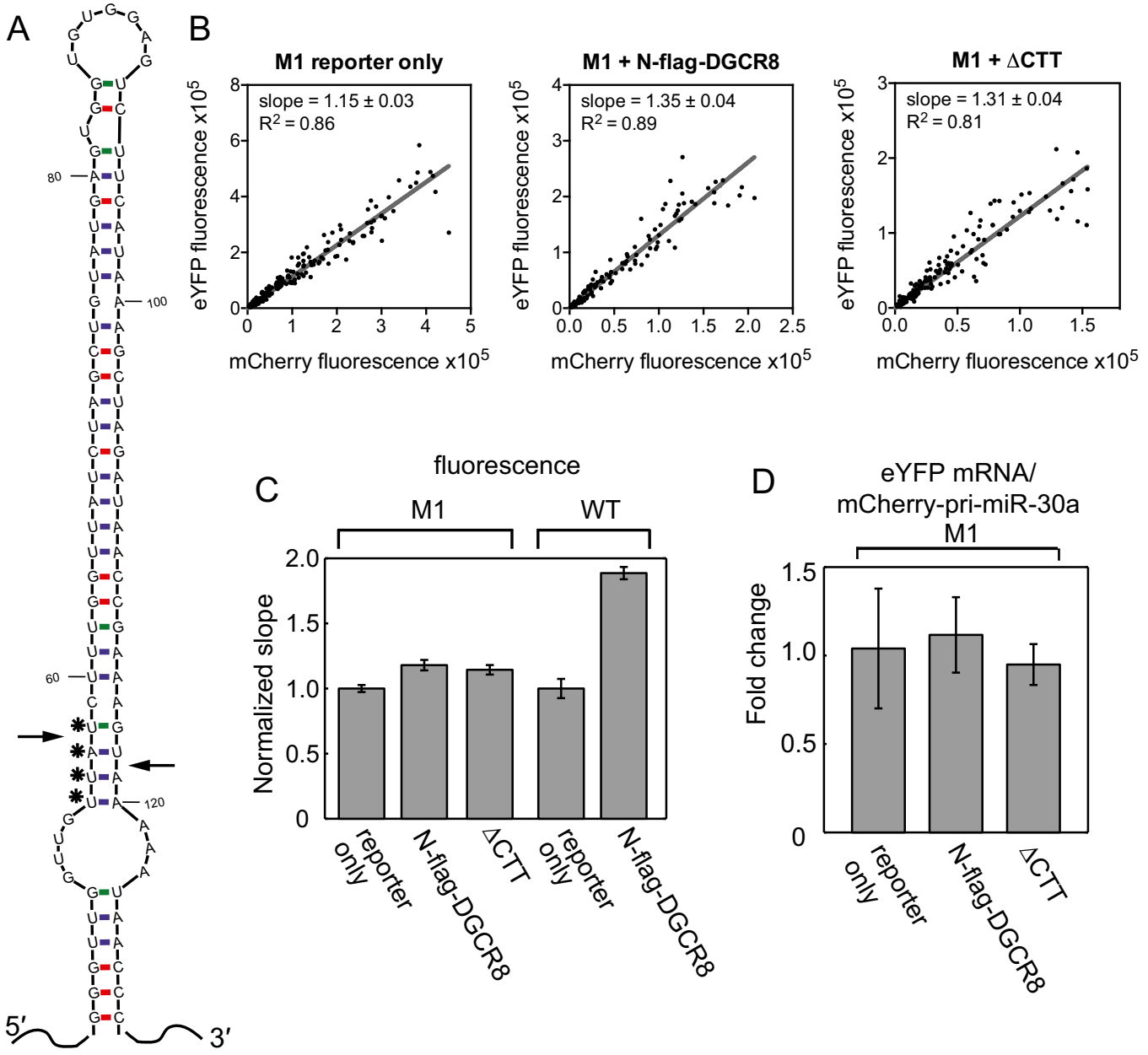

Fig. S2. Mutant pri-miR-9-1 reporter does not respond to ectopic expression of N-flag-DGCR8. (*A*) Secondary structure of the pri-miR-9-1 hairpin as predicted using MFOLD (1). Arrows indicate the expected Drosha cleavage sites. Residues marked by asterisks are mutated to AAUA (5′ to 3′) in the M1 mutant. (*B*) HeLa cells were transfected with the pri-miR-30a M1 or wild-type reporter, and pN-flag-DGCR8 plasmids as indicated. The eYFP and mCherry fluorescence signals are plotted for each cell. Slope and R^2 from linear regression are shown on the graph. The ratio of *y* and *x* axes was set at 1.6:1 for all plots. These experiments were performed together with those shown in Fig. 1*E*. (*C*) The normalized eYFP/mCherry fluorescence slopes are shown. Error bars are 95% CI from the linear fit. (*D*) qRT-PCR analyses of eYFP and mCherry-pri-miR-9-1 fusion RNAs from the experiments using the M1 reporter. Shown are average ± SD (n = 3). The slight changes, relative to the reporter-only control, are not statistically significant, with P value(N-flag-DGCR8) = 0.63 and P value(ΔCTT) = 0.93.

1. Zuker M (2003) Mfold web server for nucleic acid folding and hybridization prediction. *Nucleic Acids Res* 31(13):3406–3415.

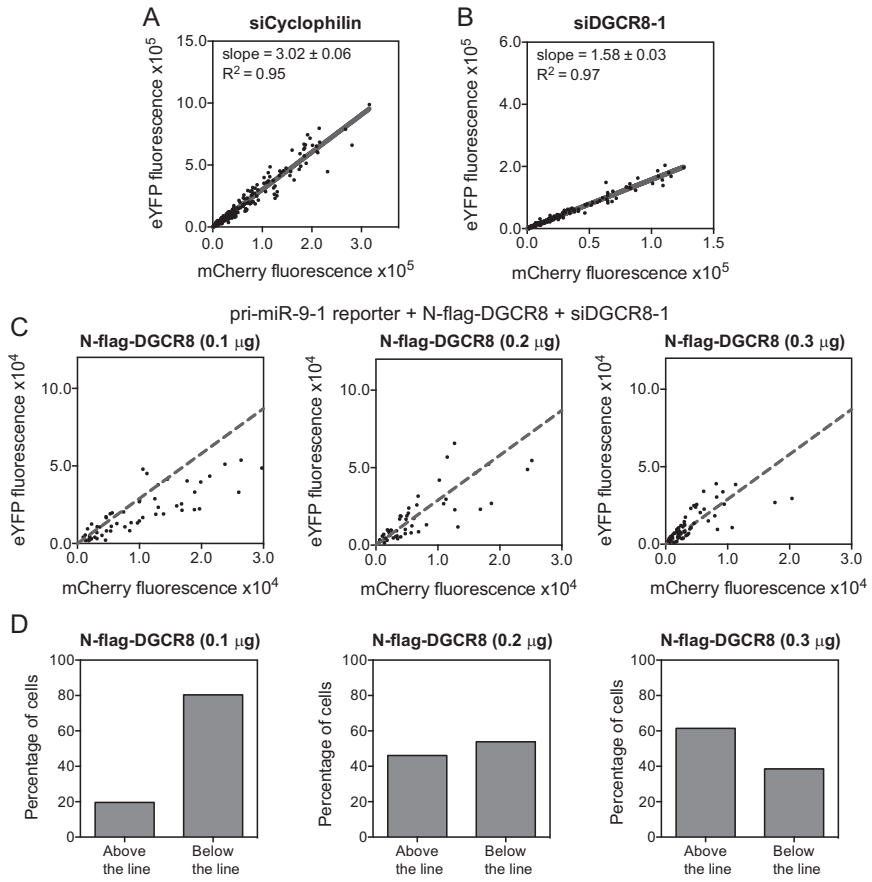

Fig. S3. Additional data to show that the reporter assay detects alteration of endogenous DGCR8 activity. (*A* and *B*) Scatter plots of eYFP vs. mCherry fluorescent intensities from the cotransfection of the pri-miR-9-1 reporter with siCyclophilin (*A*) or siDGCR8-1 (*B*), as described in Fig. 2*C*. The ratio of *y* and *x* axes was set at 4:1 for all scatter plots. (*C*) Scatter plots for cotransfections of the pri-miR-9-1 reporter, siDGCR8-1, and pN-flag-DGCR8. The amount of pN-flag-DGCR8 was varied whereas the amount of reporter was changed correspondingly to keep the total mass of plasmids to 0.4 μg, as required by the Effectene transfection protocol. The cells were assigned to the two groups based on the same gray dashed line as the linear regression fit for the data shown in Fig. 2*D* (slope = 2.9). (*D*) The percentage of data points that fell above and below the gray dashed line in *C*. We believe that cells above the line received pN-flag-DGCR8 whereas those below did not.

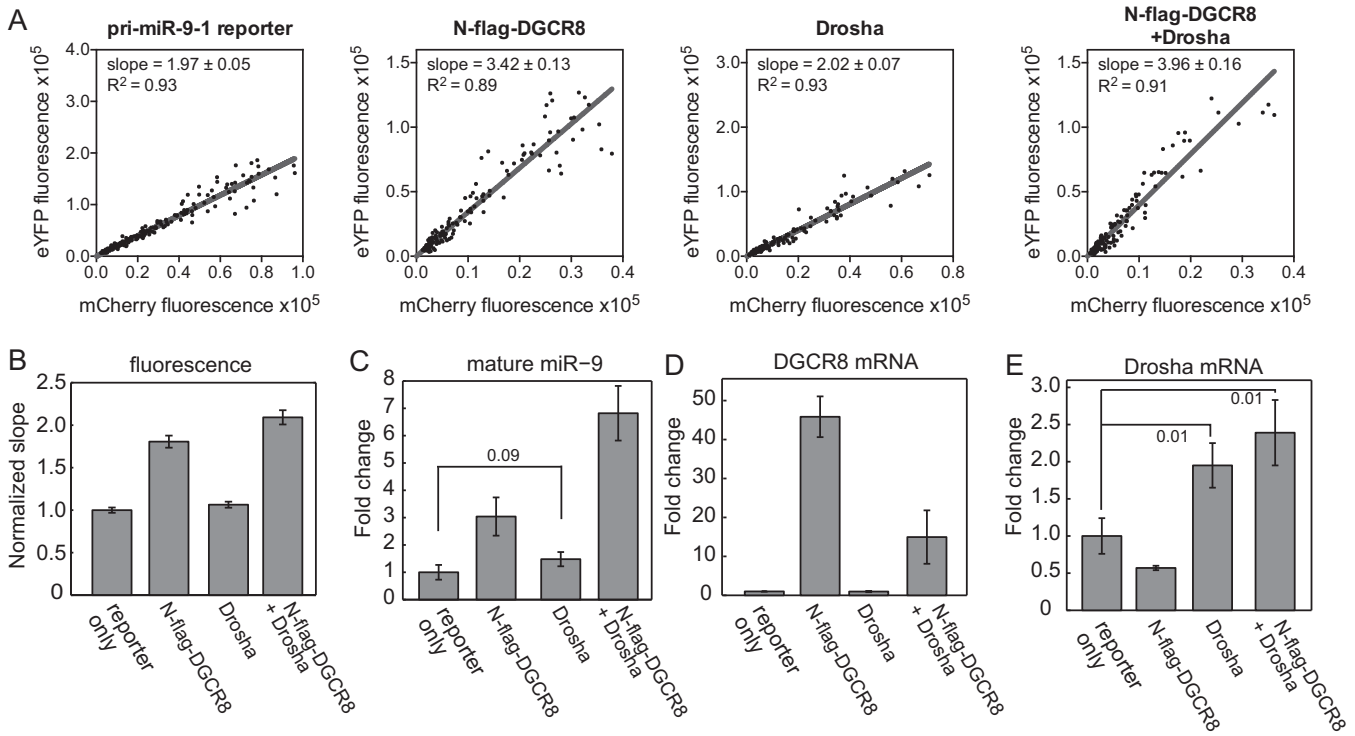

Fig. S4. Overexpression of Drosha does not enhance pri-miR9-1 processing. The pri-miR-9-1 reporter was transfected to HeLa cells either alone or with pN-flag-DGCR8, pCK-Drosha-Flag, or both. Cells were imaged, and RNA was extracted 18–20 h posttransfection. (*A*) Scatter plots showing the eYFP and mCherry fluorescence signals for individual cells and corresponding linear fits. The ratio of *y* and *x* axes was set at 4:1. (*B*) The normalized eYFP/mCherry fluorescence slope. The error bars represent 95% CI. (*C*) Mature miR-9 expression levels were measured using qRT-PCR. Error bars show SD ($n = 3$), except for N-flag-DGCR8, and "N-flag-DGCR8 + Drosha" ranges from two experiments are indicated. Total DGCR8 (*D*) and Drosha (*E*) expression levels, including expression from both endogenous genes and the plasmids, were measured using qRT-PCR. Shown are averages ± SD ($n = 3$). *P* values are labeled on the graphs.

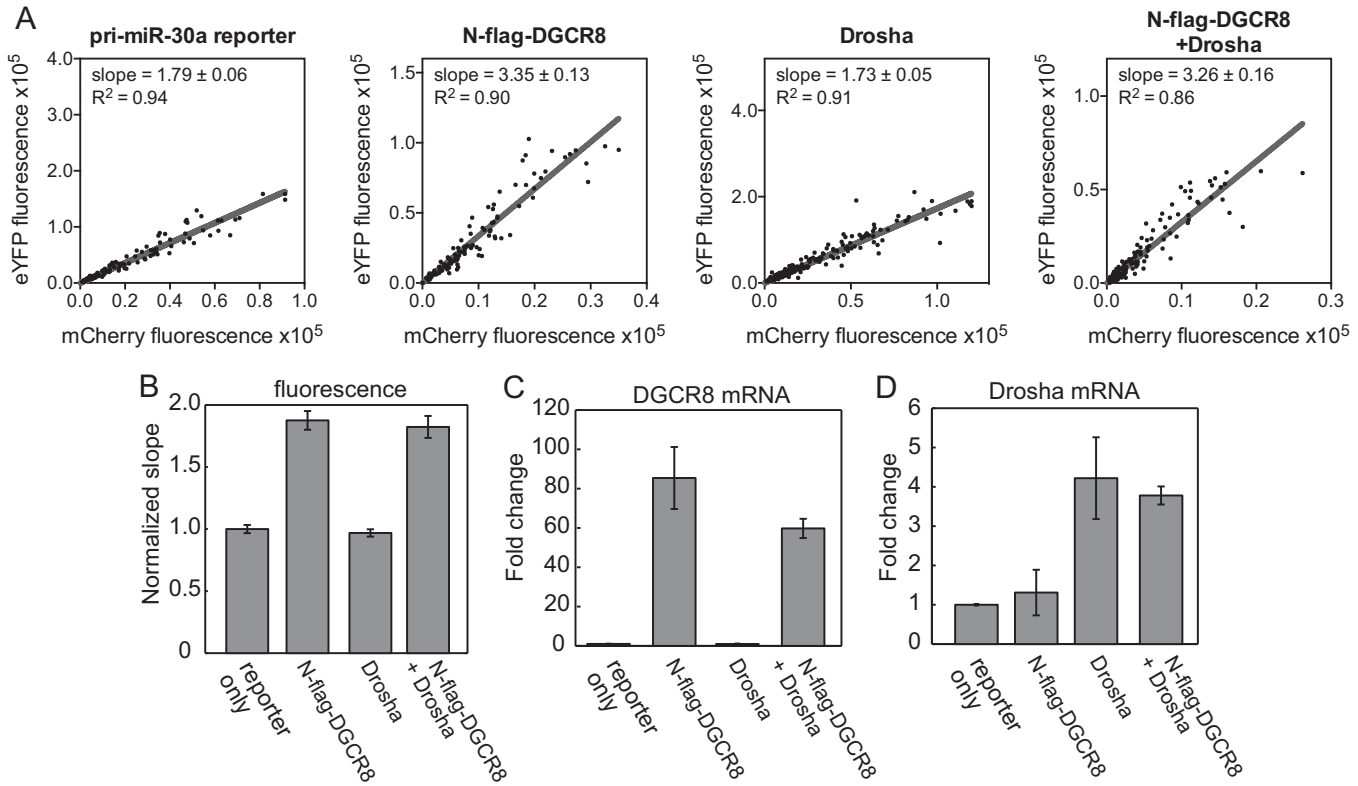

Fig. S5. Overexpression of Drosha does not enhance pri-miR-30a processing. The pri-miR-30a reporter was transfected to HeLa cells either alone or with pN-flag-DGCR8, pCK-Drosha-Flag, or both. (*A*) Scatter plots showing the eYFP and mCherry fluorescence signals for individual cells and corresponding linear fits. The ratio of *y* and *x* axes was set at 4:1. (*B–D*) The normalized eYFP/mCherry fluorescence slopes (*B*), DGCR8 (*C*), and Drosha (*D*) expression levels are plotted. Error bars in *A* represent 95% CI of the linear regression and in other panels show SD ($n = 3$).

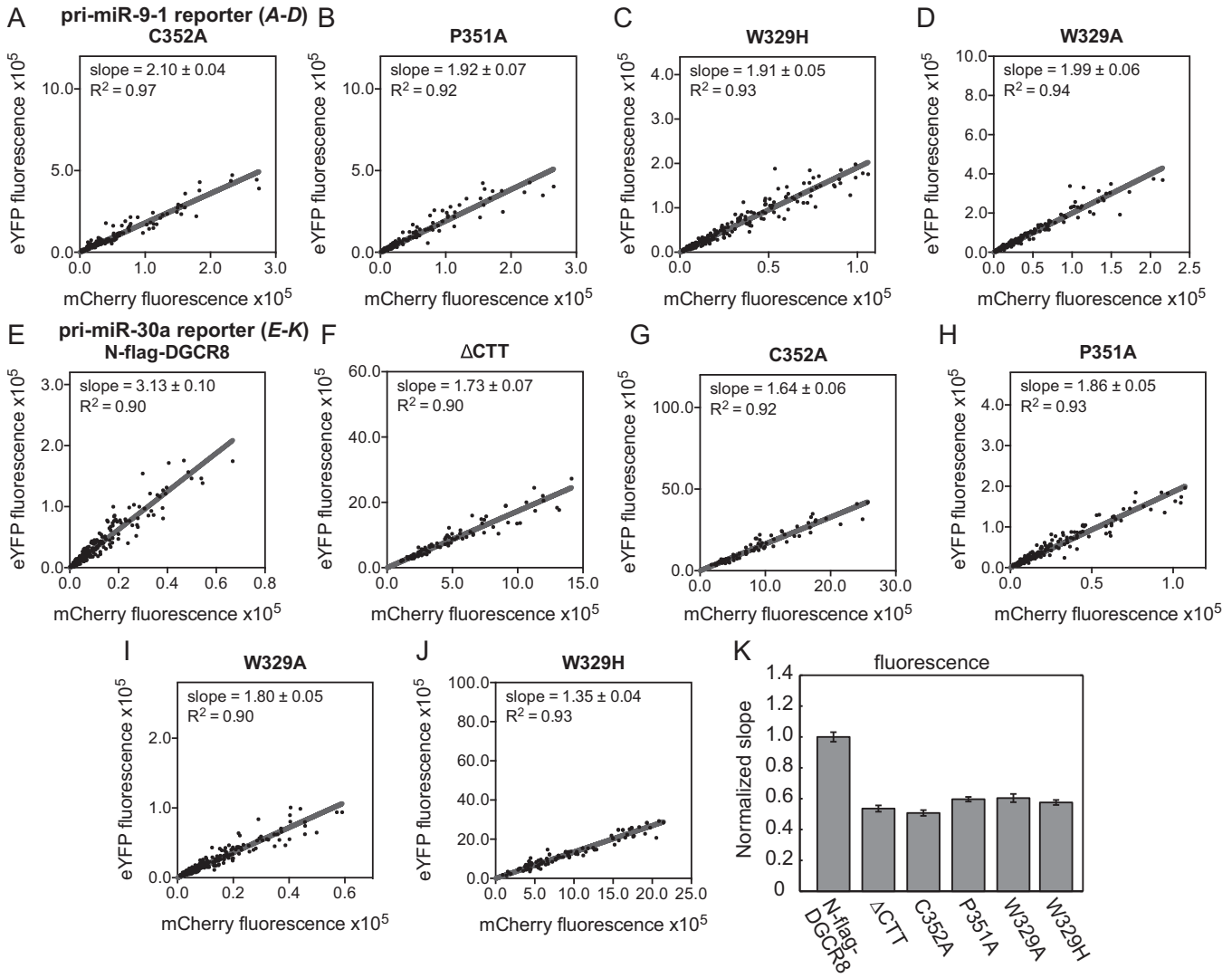

Fig. S6. All known heme-binding–deficient DGCR8 mutants are defective in cells. (*A–D*) Fluorescence scatter plots for the examination of heme-binding–deficient mutants as in Fig. 3 *A* and *F*. (*A*) C352A, (*B*) P351, (*C*) W329H, (*D*) W329A. The ratio of *y* and *x* axes was set at 4:1 for all scatter plots. Scatter plots for the corresponding N-flag-DGCR8 and ΔCTT transfections are shown in Fig. S1 *A* and *B*. (*E–K*) Examination of the DGCR8 mutants using the pri-miR-30a reporter confirms. Scatter plots of the eYFP and mCherry fluorescence signals for individual cells and corresponding linear fit for HeLa cells transfected with pri-miR-30a reporter and pN-flag-DGCR8 (*E*), ΔCTT (*F*), C352A (*G*), P351A (*H*), W329A (*I*), or W329H (*J*). (*K*) Shown are normalized eYFP/mCherry fluorescence slopes from transfections with the pri-miR-30a reporter and the indicated N-flag-DGCR8 expression plasmids. Error bars represent 95% CI from linear regression.

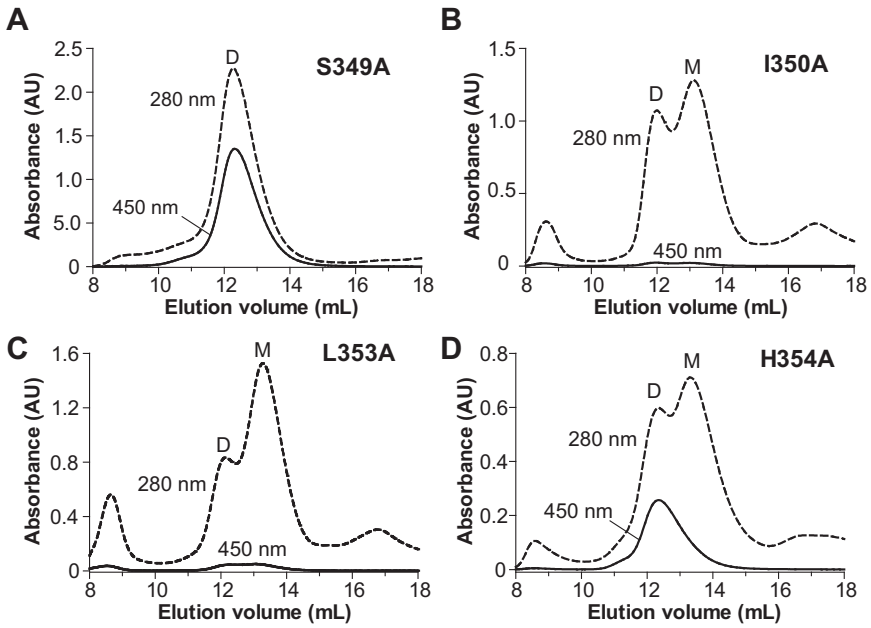

Fig. S7. Identification of a heme-binding motif in DGCR8. Mutant NC1 proteins were overexpressed in *E. coli* with 1 mM δ-ALA added at the time of induction. They were purified using a procedure described previously (5). The size exclusion chromatograms from the last step of the purification are shown. Before this step, the proteins were already over 90% pure. (*A*) S349A. (*B*) I350A. (*C*) L353A. (*D*) H354A. Dimer and "monomer" peaks are labeled as "D" and "M," respectively. The "monomer" species may not be biologically relevant, as it contains heterodimers in which one NC1 subunit is cleaved by bacterial proteases so that only the dimerization domain region remains, and the other NC1 subunit is intact.

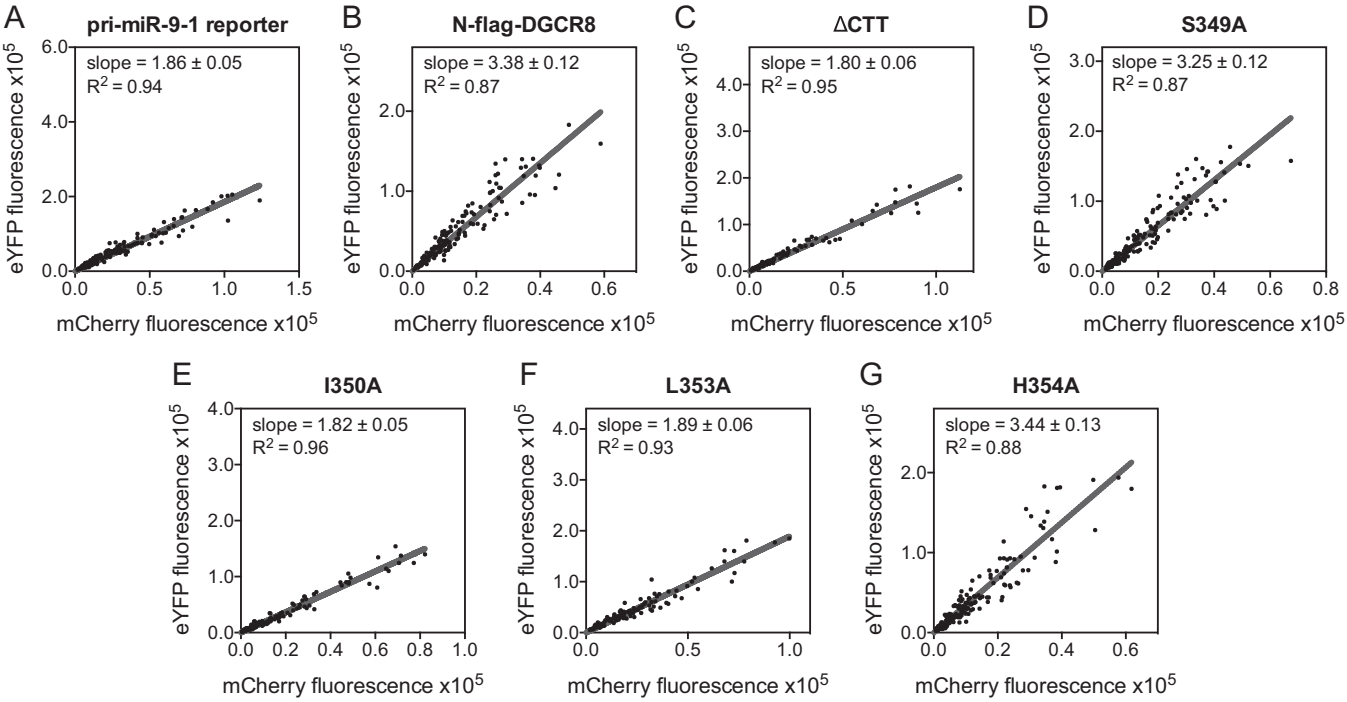

Fig. S8. Fluorescence scatter plots for the examination of DGCR8 mutations in or around the IPCL motif as in Fig. 4. The pri-miR-9-1 reporter was transfected to HeLa cells either alone (*A*) or with pN-flag-DGCR8 (*B*), ΔCTT (*C*), S349A (*D*), I350A (*E*), L353A (*F*), or H354A (*G*). The ratio of *y* and *x* axes was set at 4:1 for all plots.

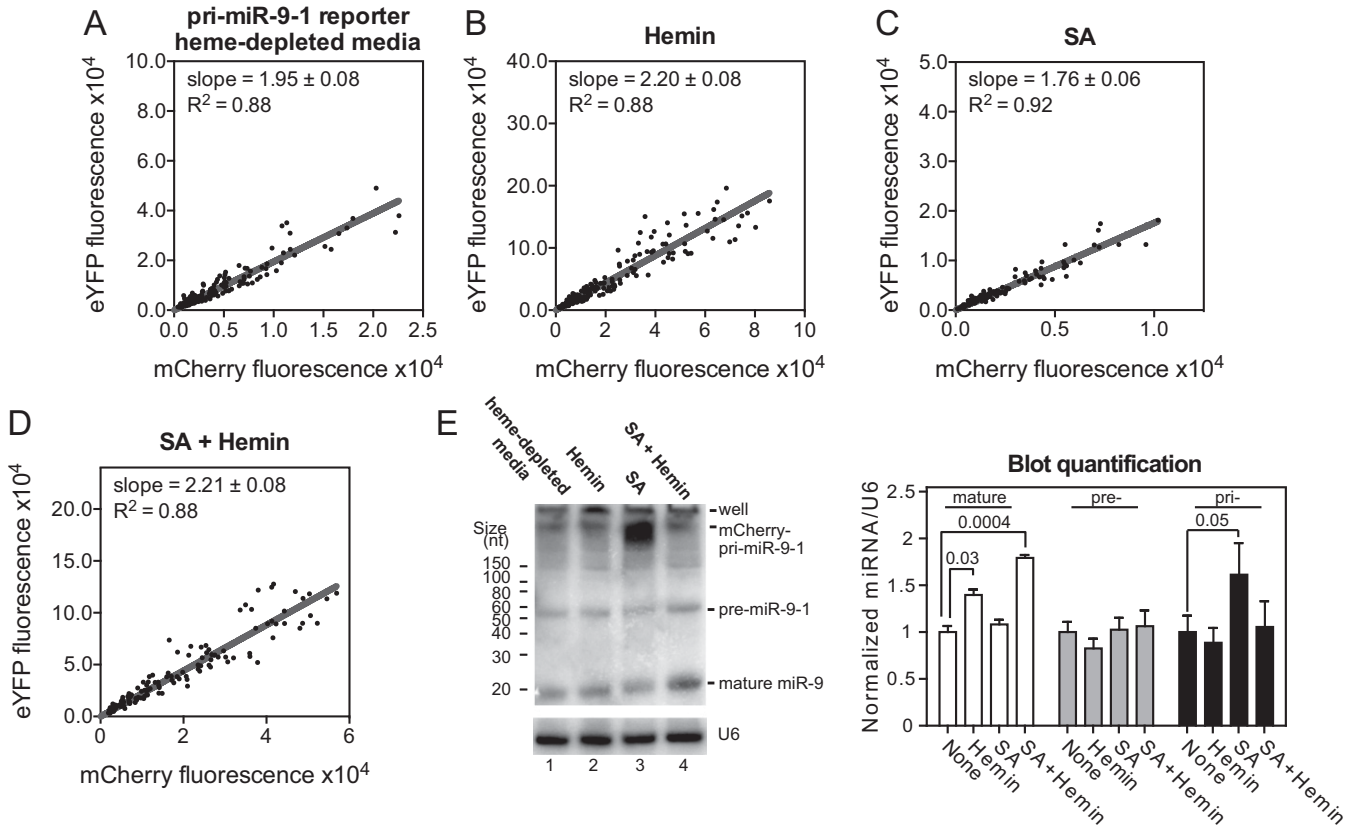

Fig. S9. Additional data to show that heme availability and biosynthesis in cells affect pri-miRNA processing. (*A*–*D*) Fluorescence scatter plots for Fig. 5*A*. HeLa cells were grown in heme-depleted media and transfected with the pri-miR-9-1 reporter, with no chemical treatment (*A*), or treated for 10 h with either hemin (*B*), or succinylacetone (*C*), or both (*D*). The ratio of *y* and *x* axes was set at 4:1 for all scatter plots. (*E*) Northern blot analyses of total RNAs. The pri-, pre-, and mature miR-9 levels, after normalization to those of U6 snRNA, are plotted on the *Right*.

Table S1. Identification of IPCL as a heme-binding motif

DGCR8 construct	Heme-bound	Heme removal by apomyoglobin	Reconstitution of heme complex
WT	Y	N	Y
S349A	Y	N	—
I350A	N	—	N
P351A	Y	Y	Y
C352A	N	—	N
L353A	N	—	N
H354A	Y	N	—

N, no; Y, yes; —, not tested.